Measuring the CO$_2$ flux at the air/water interface in lakes using flow injection analysis

F. V. Almeida,[a] **J. R. Guimarães**[b] **and W. F. Jardim**[a]

[a]*Instituto de Química, UNICAMP, Cx. Postal 6154, 13083-970 Campinas, São Paulo, Brazil. E-mail: falmeida@iqm.unicamp.br; E-mail: wfjardim@iqm.unicamp.br*
[b]*Faculdade de Engenharia Civil, UNICAMP, Cx. Postal 6021, 13083-970 Campinas, São Paulo, Brazil. E-mail: jorober@fec.unicamp.br*

The carbon dioxide flux at the air/water interface in lakes was calculated after the determination of H$_2$CO$_3$* (free CO$_2$) and atmospheric CO$_2$ using flow injection analysis (FIA) coupled to a conductometric detector. The method is based on the diffusion of CO$_2$ through a hydrophobic membrane into a flow of deionized water, generating a gradient of conductivity proportional to the concentration of CO$_2$ in the sample. Using one experimental set-up, the speciation of the inorganic carbon (H$_2$CO$_3$* and dissolved inorganic carbon) was accomplished by simply adjusting the sample pH. The determination of CO$_2$ in the atmosphere was carried out by direct injection of the gaseous samples. The FIA apparatus was taken into the field and CO$_2$ fluxes were evaluated in several Brazilian lakes. In these lakes, representing different eutrophic stages, the CO$_2$ flux varied from −242 (invasive) up to 3227 (evasive) µmol CO$_2$ m^{-2} h^{-1}.

1. Introduction

The exchange of CO$_2$ across the air/water interface is an important parameter for understanding the processes related to the carbon cycle within the aquatic environment. The direction of CO$_2$ gas exchange depends on the concentration gradient between the air and water surface, whereas the magnitude of the exchange depends additionally on the gas exchange coefficient.[1] Carbon dioxide gain and loss occur simultaneously in lakes from inputs of CO$_2$-rich underground water, variations in primary production and dissolution or precipitation of carbonate compounds within the system. In contrast to the oceans, which act mainly as net sinks for CO$_2$, freshwater systems can behave either as sinks or as sources of atmospheric CO$_2$. Data from 1835 lakes worldwide showed that 87% were CO$_2$ supersaturated with respect to the atmosphere.[2]

In the water column, CO$_2$ reacts with H$_2$O and, depending on the pH, directly with OH$^-$, producing H$_2$CO$_3$*, HCO$_3^-$ and CO$_3^{2-}$. In a closed system, the concentration of dissolved inorganic carbon (DIC) is obtained using the expression:

$$\text{DIC} = [\text{H}_2\text{CO}_3{*}_{\text{aq}}] + [\text{HCO}_3{}^-{}_{\text{aq}}] + [\text{CO}_3{}^{2-}{}_{\text{aq}}] \quad (1)$$

where

$$[\text{H}_2\text{CO}_3{*}_{\text{aq}}] = [\text{H}_2\text{CO}_3{}_{\text{aq}}] + [\text{CO}_2{}_{\text{aq}}] \quad (2)$$

Using the thermodynamic constants for carbonic acid, K_1 and K_2, eqn. (1) can be solved for H$_2$CO$_3$* as a function of pH:

$$[\text{H}_2\text{CO}_3{*}_{\text{aq}}] = \text{DIC}\{[\text{H}^+]^2/(K_1K_2 + K_1[\text{H}^+] + [\text{H}^+]^2)\} \quad (3)$$

For aqueous samples showing pH values below 8, the concentration of CO$_3^{2-}$ species is very small compared to the concentrations of the other two aqueous species (H$_2$CO$_3$* and HCO$_3^-$) present in solution, and can be neglected in a first approximation. Therefore, eqn. (3) can be rewritten as:

$$[\text{H}_2\text{CO}_3{*}_{\text{aq}}] = \text{DIC}/\{(K_1/[\text{H}^+]) + 1\} \quad (4)$$

allowing the calculation of H$_2$CO$_3$* as a function of pH.

Carbon dioxide species in aqueous solutions open to the atmosphere, and at equilibrium, are usually calculated using two out of four parameters: DIC, total alkalinity (TA), pH and the atmospheric partial pressure of CO$_2$ (pCO$_2$), together with the thermodynamic constants.[3–6] The choice is made according to the aim of the work and the facility of the measurements.[7] However, it is important to bear in mind that equilibrium conditions are rarely attained in natural water bodies and, in this situation, calculated H$_2$CO$_3$* values may differ markedly from the values obtained in realistic conditions, such as in field measurements.

The use of flow analysis for the determination of dissolved carbon dioxide by membrane separation was first reported by Carlson.[8] The method was based on the transfer of carbon dioxide by diffusion through silicone-rubber hollow fibres into a flowing stream of deionized water, followed by electrical conductivity detection. Pasquini and de Faria[9] proposed a flow injection analysis (FIA) system for the measurement of ammonia based on gas diffusion through a PTFE membrane and measurement in a conductance flow cell. Later, Jardim *et al.*,[10] based on this ammonia system, used the diffusion process to monitor aqueous CO$_2$ production from *Escherichia coli* in toxicity tests. More recently, other authors have also published articles based on the same system for the determination of DIC.[11,12]

According to a recent review by Pasquini and Silva,[13] despite the numerous papers dealing with FIA, only a few deal with the direct injection of gaseous samples. In this work, a flow injection system with a conductometric detector was developed for the determination of DIC and H$_2$CO$_3$* in aqueous samples, as well as the concentration of CO$_2$ in the atmosphere (pCO$_2$). This method introduces the novel approach of injecting gaseous samples (atmosphere) directly into the carrier.

Initially, the whole experimental set-up was evaluated according to its ability to measure H$_2$CO$_3$*, and consequently DIC, in a closed reactor, at known conditions (pH and ionic strength). Later, using the optimized set-up in the field, the determination of H$_2$CO$_3$* and pCO$_2$ was carried out *in situ* and without disturbing the natural condition of the sample. The major advantage of the proposed method is that the speciation

of inorganic carbon in aqueous samples is carried out experimentally and not inferred with the use of thermodynamic parameters. In addition to this, the same system set-up also allows the injection of gaseous samples to accomplish the determination of atmospheric CO_2.

2. Experimental

2.1. Reagents

Water used in the conductivity experiments was obtained from a Milli-Q reagent-grade water system (Millipore Corp.). The H_2SO_4 solution and the stock solution of $NaHCO_3$ were prepared from analytical grade reagents (Merck, Germany). The working reference $NaHCO_3$ solutions were prepared by dilution of the stock solution just before use.

2.2. Apparatus and experimental set-up

The system manifold is shown in Fig. 1. The experimental procedure is based on the previous work of Pasquini and de Faria[9] and Jardim et al.,[10] where specific details about laboratory-made components are provided. Basically, the method is based on the diffusion of CO_2 through a non-wetting, gas porous membrane (PTFE) that is supported by an acrylic cell (diffusion cell). The permeating gas is collected in a stream of freshly distilled and deionized water (the acceptor stream) that flows towards a microconductivity cell (40 µL volume). The conductivity meter (Micronal B372) output is plugged to a strip-chart recorder (Cole-Parmer 8376-20). A peristaltic pump (Ismatec MS-Reglo, four channels, and variable speed) is used to circulate the fluids at a flow rate of 2.5 mL min^{-1}. The injection valve (V) is used to insert both gaseous and aqueous samples into the system. The system allows the injection of non-perturbed samples, yielding values of $H_2CO_3^*$, acidified samples, yielding values of DIC, and gaseous samples in the determination of atmospheric CO_2.

2.3. Calibration of the FIA for $H_2CO_3^*$ measurements

For performing direct measurements of dissolved CO_2, the experimental set-up was first coupled to a headspace-free reactor containing sodium bicarbonate solution. In this set-up, the injection valve, shown in Fig. 1, was removed and the glass piston reactor was connected directly to the donor stream. Fig. 2 shows the 700 mL volume reactor made of borosilicate glass and containing three different apertures. The first aperture was used to insert the glass-combined electrode (Orion, 8104 Ross) for continuous pH measurements. The second aperture was used to withdraw the solution to the FIA system, and the third was used to add known volumes of 0.5 mol L^{-1} H_2SO_4 in order to alter the solution pH towards more acidic values. The reactor with a glass piston acted as a

Fig. 2 Headspace-free reactor used in the determination of $H_2CO_3^*$ using standard bicarbonate solutions.

reservoir and allowed the sampling of up to 50 mL of solution without the formation of headspace.

The calibration involved changing the pH of the $NaHCO_3$ solution and reading the CO_2 values until no further changes in the conductivity were noticed. After reaching the steady state, new addition of acid was made and the system was allowed to equilibrate, generating a new value for the CO_2 concentration. The final shape of the register is a staircase form (Fig. 3a).
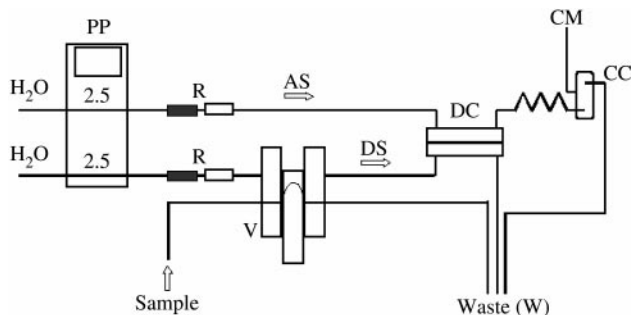

Fig. 1 Flow manifold used in the inorganic carbon speciation (reagent injection mode) and atmospheric CO_2 measurement: peristaltic pump (PP); sample or standard introduction valve (V); mixed-bed resins (R); diffusion cell (DC); conductance cell (CC); conductivity meter (CM); waste (W); acceptor stream (AS); and donor stream (DS).
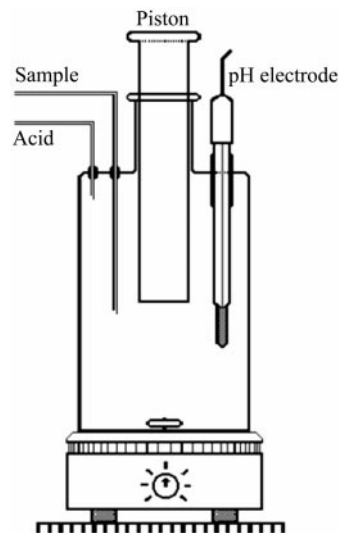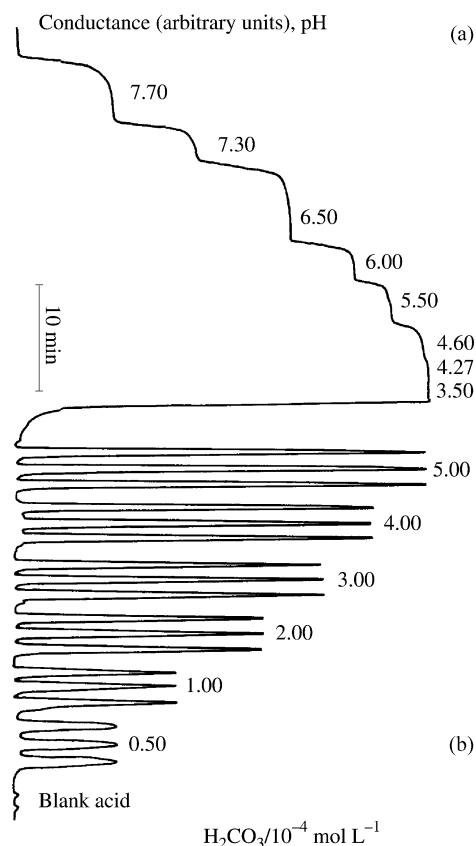

Fig. 3 (a) Calibration curve in the staircase form. Results obtained using the headspace-free reactor. The numbers above each step indicate the measured pH. (b) Calibration curve obtained through injection of standards for three replicates of different bicarbonate standard solutions.

During the pumping of the bicarbonate solution to the diffusion cell, a headspace-free system was ensured by the presence of the piston. When the pH inside the reactor reached values below 4, the concentration of $H_2CO_3^*$ equalled the value attained for DIC. Considering this closed system, experimental values obtained for $H_2CO_3^*$ could be compared with theoretical ones obtained using pH, K_1 and the ionic strength.

2.4. Sampling locations and methodology

Sampling was carried out in four Brazilian lakes: Lake Tupé (60°15′ W, 03°03′ S) and Calado (60°34′ W, 03°15′ S), both marginal lakes of the Amazonas River; Óleo Lake (47°50′ W, 21°35′ S), a marginal lake of the Mogi-Guaçu River, São Paulo State; and Taquaral Lake (47°03′ W, 22°52′ S), an artificial and hypereutrophic lake in the city of Campinas, São Paulo State.[14] The FIA system was transported to the field, close to the sampling points, in order to allow *in situ* analysis.

Óleo Lake, a waterflood basin, was sampled four times on each survey day in order to evaluate diurnal variation in both pCO_2 and $H_2CO_3^*$. The first sampling was performed in October 1997 (cold and dry season), and the second in March 1998 (hot and rainy season). Water samples from Óleo Lake were also collected at different depths, with a Kemmerer bottle. Amazonian lakes were sampled during the wet season (in May 1997) when the lake depths reached 10 m. Taquaral Lake was sampled three times in October 1997, during one day.

Surface water samples were collected in a 60 mL plastic (polyethylene) syringe, taking special care to keep a headspace-free condition; the atmosphere was also sampled with 60 mL plastic syringes, through 30 m polyethylene tubing (id, 1.5 mm) fixed in a floating device, in order to avoid interference caused by the CO_2 exhaled by the sampler. Almeida[15] established that gaseous and aqueous samples collected and stored in polyethylene syringes and equipped with a three-way valve suffered no change in $H_2CO_3^*$ and pCO_2 for a period shorter than 3 h. Air samples were injected directly into the unit's injection valve from the syringes, where the sample loop in the injection valve was responsible for ensuring the same volume of sample to be used in the CO_2 determination.

3. Results and discussion

3.1. Checking the FIA performance for measuring aqueous CO_2

The preliminary steps of the experimental procedure involved the validation of the system to perform inorganic carbon speciation. The headspace-free reactor was fully filled with a solution containing 5.00×10^{-4} mol L^{-1} NaHCO$_3$ and 0.05 mol L^{-1} NaNO$_3$ to adjust the ionic strength. Keeping the temperature constant at 22 °C, the solution was submitted to a rapid mixing, after the addition of 15 µL of 0.1 mol L^{-1} H$_2$SO$_4$, using a 2000 µL microburette. On acidification, the amount of CO_2 crossing the PTFE membrane increases as a consequence of the carbonate equilibrium. This causes an increase in the conductivity of the deionized water stream receiving the diffused CO_2. As a consequence, the monitored signal increases and reaches a plateau. This situation is only changed on new addition of acid, as already discussed in Section 2.3.

The concentration of $H_2CO_3^*$ in Fig. 3a was experimentally determined using this experimental set-up and compared with the theoretical values expected for the experimental conditions used (pH, NaHCO$_3$ concentration and the equilibrium constants at the selected temperature and ionic strength). When theoretical and experimental $H_2CO_3^*$ values are plotted against pH (Fig. 4), both curves show excellent agreement, thus validating the proposed method.
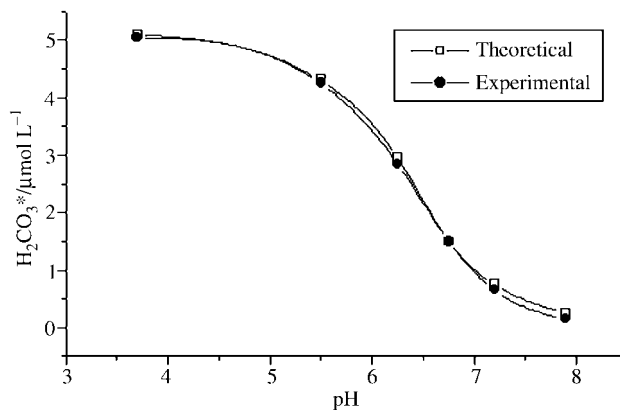

Fig. 4 Theoretical and experimental $H_2CO_3^*$ against pH using the headspace-free reactor. Conditions: $T = 22$ °C; p$K_1 = 6.38$; $I = 0.05$ mol L^{-1}; NaHCO$_3 = 5 \times 10^{-4}$ mol L^{-1}.

3.2. Optimizing the system for field measurements of CO_2

The system had to be optimized in order to measure both aqueous and gaseous samples using the same experimental set-up. The main difference between measuring aqueous and gaseous CO_2 is the amount of gas permeating the diffusion cell. For pCO_2 determination, the amount of CO_2 crossing the membrane is very low compared to that for aqueous samples. For this reason, a 60 cm long PTFE reaction coil (id, 0.8 mm) was placed between the permeation and conductivity cell (CC) to increase the hydration time of the CO_2 and thus to improve the sensitivity. Two columns of ion exchange resins (cationic and anionic) were also introduced in both donor and acceptor streams (see Fig. 1) to decrease the baseline conductivity signal and, consequently, increase the sensitivity. The flow rate was maintained at 2.5 mL min^{-1} for both donor and acceptor streams because it generated better analytical throughput and sensitivity for both gaseous and aqueous samples.

3.3. Measuring gaseous CO_2

Measurements of gaseous CO_2 were performed with the help of a calibration curve constructed using a simple gas dilution procedure. Initially, a 2.0 L Erlenmeyer flask was calibrated by using the classical analytical procedure of glassware calibration through the water density. The flask was flushed with nitrogen and sealed with a rubber septum. Before any CO_2 addition, around 2 mL of this CO_2-free atmosphere was collected from the Erlenmeyer flask, using a 3 mL plastic (polyethylene) syringe, and injected directly from the syringe into V (injection valve from the FIA system, Fig. 1), creating a gaseous segment in the carrier stream and generating the blank signal. Each injection was repeated three times.

The calibration curve was generated by adding previous selected volumes of gaseous CO_2, using a 500 µL gas-tight syringe, to the calibrated Erlenmeyer flask containing nitrogen, followed by injection in the FIA system (as described above). The gaseous CO_2 was obtained by simply placing around 10 g of solid (99.9% pure) CO_2 in a small flask (250 mL), partially covered with polyethylene film, which saturated its atmosphere due to sublimation of the solid.

The sampling volume injected was 300 µL (easily adjusted according to the sample loop size in the valve V) in order to improve sample throughput and avoid peak distortion due to insufficient mixing in the acceptor stream. Under these conditions, the analytical frequency in the field was 48 h^{-1}. The detection limit, calculated according to Miller and Miller,[16] was 10 µmol L^{-1} with a relative standard deviation of 1.8% when working with 300 µL of sample ($n = 15$), which can be considered to be very suitable for the measurement of CO_2 flux at the water/air interface.

3.4. Measuring DIC and H₂CO₃*

An analytical calibration curve was constructed by adding a few millilitres of H_2SO_4 to a series of $NaHCO_3$ analytical solutions (50–500 µmol CO_2 L^{-1}) until pH 3.5 just before injecting the sample. In this procedure, the conductivity signal appears in the shape of a peak and not as that previously described (Fig. 3b). A quadratic (rather than a linear) equation describes the signal response as a function of carbon concentration due to the behaviour of H_2CO_3 as a weak electrolyte.

The injection volume used in the determination of $H_2CO_3^*$ was optimized to 1000 µL, the minimum volume necessary to reach steady state conditions for the non-perturbed samples. Results obtained using this procedure refer to the concentration of $H_2CO_3^*$. In the determination of DIC, 50 mL of sample was filtered using 0.45 µm membrane (Millipore), and a few millilitres of H_2SO_4 were added immediately prior to sample injection. The injection volume was 150 µL.

Based on the optimized conditions, the flow system showed a sampling frequency of 45 h^{-1} for DIC and 30 h^{-1} for $H_2CO_3^*$. The detection limit was 3 µmol L^{-1} with a relative standard deviation of 1.2% when working with a sample volume of 1000 µL ($n=20$) for $H_2CO_3^*$. For DIC, the detection limit was also 3 µmol CO_2 L^{-1} with a relative standard deviation of 1.9% when working with a sample volume of 150 µL ($n=6$).[16]

Positive interference in DIC measurements may be caused by volatile organic and inorganic acids and oxides able to permeate the PTFE membrane and dissociate (mainly formic and acetic acid, H_2S, NO_2 and SO_2). For $H_2CO_3^*$, due to the fact that the pH is not adjusted to values below 4 prior to the measurements, ammonia and volatile organic bases may cause interference. These compounds, however, are usually present in such low concentrations that they pose no bias when compared to the inorganic carbon species present in natural waters.

3.5. Empirical flux equations

Gaseous carbon dioxide is very soluble in water. It follows Henry's law under low partial pressure and concentrations:

$$[pCO_2] = K_H[H_2CO_3^*]_{eq} \qquad (5)$$

where K_H is Henry's constant and pCO_2 is the partial pressure of CO_2 at equilibrium with $H_2CO_3^*$ in the water body. Using the global average pCO_2 value (356 ppmv) and considering $K_H = 3.39 \times 10^{-2}$,[17] one should expect $H_2CO_3^*$ to be 1.21×10^{-5} mol L^{-1}.

The transfer of CO_2 between the gas phase (i.e. air) and water, when the two phases are in contact, will depend mainly on the gradient of CO_2 at this interface. The water/air interface can be considered as a stagnant boundary layer, and the transport from the water to the air, or vice versa, is governed by Fick's law [eqn. (6)]:

$$F = K[C^{atm} - C^{aq}] \qquad (6)$$

where K is the gas transfer velocity and the term in square brackets is the difference in CO_2 concentration between the two phases.

For CO_2, a reactive gas, the gradient across the air/water interface will not always be constant, especially for natural waters with high pH values, since the reaction of dissolved CO_2 with OH^- ions is expected. For this reason, the theoretical calculation involving the transport of CO_2, which takes into account the diffusion and reactive processes, is a time-consuming and complex task. When working with natural systems, instead, the use of empirical flux equations is a suitable option to overcome this problem. In this case, the parameters to be determined are the concentrations of CO_2 in water and in

air, the temperature of the upper water layer and the wind velocity at the water surface.

For unenhanced exchange, many empirical equations for transfer velocity have been proposed in the literature. In this work, the equation proposed by Wanninkhof et al.[18] is used, which is dependent on the wind speed according to:

$$K_{CO_2} = 0.76\mu[600^{0.67}/(Sc_{CO_2})^{0.67}], \text{ for } \mu < 3 \text{ m s}^{-1} \qquad (7)$$

$$K_{CO_2} = ((5.6\mu) - 14.4)[600^{0.5}/(Sc_{CO_2})^{0.5}], \text{ for } \mu > 3 \text{ m s}^{-1} \qquad (8)$$

where Sc is the Schmidt number for CO_2 at 20 °C and μ is the wind velocity measured at the water surface.

3.6. Flux calculations

The major problem concerning the use of eqn. (4) for the speciation of aqueous CO_2 is that K_1 values are not always available, especially when the ionic strength is not known with accuracy. Furthermore, for freshwater samples, the low ionic strength and sample exposure to the atmosphere may cause errors in pH readings mainly due to the slow response of the electrode, markedly affecting the values of the theoretically calculated $H_2CO_3^*$.[19]

In spite of all the corrections that can be made to minimize the errors associated with the equilibrium constants and the pH measurements, many authors still observe deviations in $H_2CO_3^*$ when compared to the values obtained from alkalinity measurements. For example, Butler and Mackey[4] carried out an evaluation of pCO_2 via pH and alkalinity in the Tasman Sea and around New Zealand. The data obtained using the pH values and the alkalinity calculated from the surface salinity were approximately 20 µmol L^{-1} lower than those obtained using an infrared gas analyser. On the other hand, Frankignoulle et al.[20] carried out a study in a polluted estuary (the Scheldt), using pH and total alkalinity measurements to calculate $H_2CO_3^*$ (expressed as pCO_2^{aq}) in the water column, and observed lower errors. They ranged from 6 µatm, in seawater, to 65 µatm (2.9 µmol L^{-1}, expressed as $H_2CO_3^*$) in freshwater.

According to the results obtained in the present work, Óleo Lake is supersaturated with $H_2CO_3^*$ compared to the overlying atmosphere (Fig. 5). From the measurements carried out in two surveys, the mean value for CO_2 in surface water was 7977 ± 4045 µatm. The values of $H_2CO_3^*$ have been converted to µatm following the tendency observed in the literature.[1,20] The diurnal variation in $H_2CO_3^*$ in the two surveys was small in comparison to the CO_2 supersaturation. In both cases, measurements over a 24 h period failed to indicate any significant diurnal variation in CO_2. On the other hand, it is apparent that supersaturation is a depth-related phenomenon
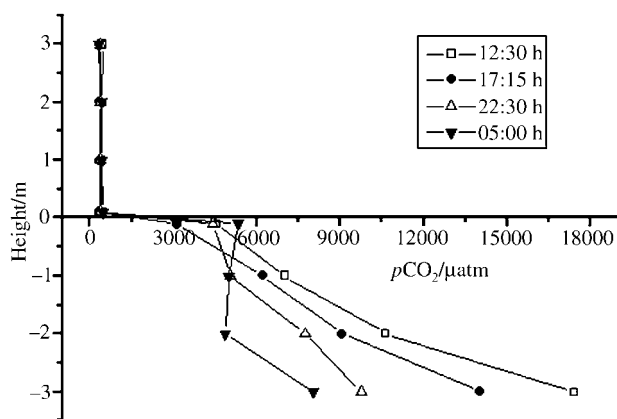

Fig. 5 pCO_2 in the water and air from Óleo Lake measured in October (cold and dry season). The height at 0 m represents the water surface.

Table 1 Some physicochemical characteristics and measured CO_2 flux as a function of time across the water/air interface of Lake Taquaral

Characteristic	Time			Average value
	6:30 h	10:45 h	15:30 h	
pCO_2^{aq}/µatm	45 ± 1	13 ± 1	10 ± 1	23 ± 19
pCO_2^{atm}/µatm	422 ± 1	392 ± 3	450 ± 2	421 ± 29
pH	9.1	9.5	9.6	9.4 ± 0.3
DO/mg O_2 L^{-1}	9.9	11.8	12.5	11.4 ± 1.4
Flux/µmol CO_2 m^{-2} h^{-1}	-105	-116	-142	-121 ± 19

Table 2 CO_2 partial pressure and estimated flux across the water/air interface for some Brazilian lakes

Lake	pCO_2^{atm}/ µatm	pCO_2^{aq}/µatm	Flux/ µmol CO_2 m^{-2} h^{-1}
Tupé	421 ± 5	3187 ± 29	3227
Calado	464 ± 8	1121 ± 22	1852
Óleo (October, 1997)	389 ± 50	4355 ± 900	1081
Óleo (March, 1998)	427 ± 26	11599 ± 1543	3383

and the probable causes of this supersaturation at depth are the production of CO_2 by sediment microbial respiration and the influx of CO_2-rich underground water.[21]

The two Amazonian lakes sampled are representative of so-called black waters: low pH values (average pH 4.7) and high dissolved organic carbon (DOC), with average values around 15 mg C L^{-1}. In these waters, humic materials act as proto-lytes, thus altering the values of DIC obtained *via* alkalimetric titration. The H_2CO_3* values obtained were much higher than the value expected for atmospheric equilibrium. Consequently, these lakes are acting as a source of CO_2 to the atmosphere.

Taquaral Lake was the only sampled reservoir that showed undersaturated CO_2 values, relative to the overlying air. Based on H_2CO_3*, dissolved oxygen data (9.9–12.5 mg O_2 L^{-1}) and gaseous CO_2 in the overlying air, at three different periods in a day (Table 1), this hypereutrophic reservoir may be acting as a sink for gaseous CO_2. In addition, the increase in the evasive flux is a function of solar radiation intensity, *e.g.* primary production.

The data from fieldwork showed that, in all the oligotrophic lakes studied, the concentration of dissolved CO_2 was always higher than the expected value, assuming equilibrium with atmospheric CO_2, indicating that they are supersaturated in relation to the overlying atmosphere. Table 2 shows the calculated CO_2 flux across the water/air interface from the other three sampled lakes (Tupé, Calado, Óleo).

As expected, the results show that CO_2 equilibrium is seldom attained, principally due to physical, biological and chemical factors that affect the concentration and exchange of CO_2 between the air and water phases.[6] According to Cole *et al.*,[2] only 7% of a total of 1835 lakes investigated were within $\pm20\%$ of equilibrium with the atmosphere, and 87% were supersaturated.

4. Conclusions

The proposed flow analysis system is characterized by a simple set-up, an inexpensive apparatus and ease of operation. It can be adapted to perform fieldwork and *in situ* measurements. The principal advantages of this system are the possibility to perform inorganic carbon speciation in natural waters without the need to know the sample pH and the relevant thermodynamic constants, and the fact that it uses only low-cost, stable reagents (deionized water and H_2SO_4).

It should also be mentioned that the possibility of measuring *in situ* both aqueous and gaseous CO_2 using the same system manifold is important in flux studies at the water/air interface of natural reservoirs.

All the lakes studied were far from thermodynamic equilibrium, either showing supersaturation or undersaturation. Furthermore, the undersaturation condition was obtained only for a hypereutrophic lake where positive (invasive) CO_2 fluxes were generated.

Acknowledgements

References

1 J. J. Cole and N. F. Caraco, *Limnol. Oceanogr.*, 1998, **43**, 647.
2 J. J. Cole, N. F. Caraco, G. W. Kling and T. K. Kratz, *Science*, 1994, **265**, 1568.
3 T. Takahashi, *Oceanus*, 1989, **29**, 22.
4 E. C. V. Butler and D. J. Mackey, *Sci. Total Environ.*, 1992, **112**, 165.
5 A. Poisson, F. Culkin and P. Ridout, *Deep-Sea Res.*, 1990, **37**, 1647.
6 C. Goyet, D. R. Walt and P. G. Brewer, *Deep-Sea Res.*, 1992, **39**, 1015.
7 T. Takahashi and P. Kaiteris, *Earth Planet. Sci. Lett.*, 1976, **32**, 451.
8 R. M. Carlson, *Anal. Chem.*, 1978, **50**, 1528.
9 C. Pasquini and L. C. de Faria, *Anal. Chim. Acta*, 1987, **193**, 19.
10 W. F. Jardim, C. Pasquini, J. R. Guimarães and L. C. de Faria, *Water Res.*, 1990, **24**, 351.
11 T. Aoki, Y. Fujimaru, Y. Oka and K. Fujie, *Anal. Chim. Acta*, 1993, **284**, 167.
12 P. O. J. Hall and R. C. Aller, *Limnol. Oceanogr.*, 1992, **37**, 1113.
13 C. Pasquini and M. C. H. Silva, *J. Braz. Chem. Soc.*, 1999, **10**, 85.
14 J. T. Borges, MSc Thesis, Universidade Estadual de Campinas, Brazil, 1998.
15 F. V. Almeida, Master Thesis, University of Campinas, Brazil, 1998.
16 J. C. Miller and J. N. Miller, *Statistics for Analytical Chemistry*, Ellis Horwood Ltd., New York, 1984, p. 99.
17 W. Stumm and J. J. Morgan, *Aquatic Chemistry*, Wiley-Interscience Publication, New York, 3rd edn., 1996, p. 214.
18 R. Wanninkhof, J. R. Ledwell and J. Crucius, in *Air Water Gas Transfer*, ed. S. C. Wilhelms and J. S. Gulliver, American Society of Civil Engineers, New York, 1991, p. 441.
19 W. F. Jardim, J. R. Guimarães and H. E. Allen, *Ciênc. Cult.*, 1991, **43**, 454.
20 M. Frankignoulle, I. Bourge and R. Wollast, *Limnol. Oceanogr.*, 1996, **41**, 365.
21 A. A. Mozeto and A. L. S. Albuquerque, *Ciênc. Cult.*, 1997, **49**, 25.